Transp Porous Med (2008) 71:5–22
DOI 10.1007/s11242-007-9108-5

ORIGINAL PAPER

Experimental displacement patterns in a 2 × 2 quadrant block with permeability and wettability heterogeneities—problems for numerical modelling

Richard A. Dawe · Carlos A. Grattoni

Received: 23 May 2006 / Accepted: 19 January 2007 / Published online: 13 April 2007

Abstract The effect of heterogeneities on miscible and immiscible flood displacements in 2D bead packs in quadrant form, 2 × 2 block heterogeneity, with either a permeability or a wettability contrast is the subject of this paper. The physical processes occurring during miscible and immiscible flow and displacement within permeability and wettability quadrant bead pack models have been studied experimentally. This geometry occurs in a number of situations relevant to hydrocarbon production: particularly faults where adjacent rocks have large permeability contrasts with rapid changes, in the laboratory with core butting, in reservoir simulation where grid blocks have different permeability and in reservoirs having near-wellbore damage problems. The model quadrants 1–4, had 1 and 4 and 2 and 3 with identical properties, either in permeability or wettability. Reported are complete unit mobility miscible displacements, then the effects of viscosity differences (mobility modifiers) and finally immiscible displacements on displacement patterns for initial linear injection. The experiments demonstrate that nodal flow occurs for both miscible and immiscible flow, but for immiscible flow there are boundary effects due to capillary pressure differences created by water saturation changes or wettability contrasts which can leave patches of isolated fluid within a quadrant. The displacement patterns for the different models and fluids change significantly with the viscosity and wettability changes, particularly for the immiscible displacements. This is due to the changing capillary pressure between the quadrant blocks as the water saturation change. These are difficult to address in numerical modelling but should be accounted for. Other

R. A. Dawe (✉)
Department of Chemical Engineering, The University of the West Indies,
St. Augustine, Republic of Trinidad and Tobago
e-mail: radawe@eng.uwi.tt

C. A. Grattoni
Rock Deformation Research Limited (RDR), Earth Sciences,
University of Leeds,
Leeds LS2 9JT, UK
e-mail: carlos@rdr.leeds.ac.uk

effects include coupling of all physical processes governing the flow through the node (viscous, interfacial, gravity etc. forces) and creations of microzones of trapped residual oil. Our displacement patterns can therefore be a valuable verification benchmark tool for numerical modelling and a calibration data source for those wishing to simulate the effects of capillary pressure under differing wettability conditions and for those investigating upscaling modelling procedures. However, the possible loss of physical reality when averaging must always be considered.

Keywords Quadrant model · Heterogeneity · Upscaling · Renormalisation · Flow mechanisms · Miscible displacement · Immiscible displacement · Wettability · Capillary pressure · Imbibition · Drainage · Reservoir simulation

1 Introduction

All natural hydrocarbon reservoirs are heterogeneous, as the rock properties such as permeability, porosity and wettability vary over the reservoir and at all length scales. An understanding of the movement of fluids within such heterogeneous porous media is fundamental to petroleum production prediction and efficient reservoir management. It also has relevance to Non-Aqueous Phase Liquids (NAPL)-contaminated porous media, particularly aspects of flow, transport and remediation (Chevalier and Petersen 1999). These heterogeneities cause non-uniform fluid distributions and irregular displacement patterns, as the oil is displaced from the pores within the rocks during hydrocarbon production. If the effects of heterogeneities are not well accounted for at the planning stage of an operation, any negative effects may become evident when it is too late.

Wettability heterogeneities also occur in reservoir rocks, however, their effects on displacement efficiency and oil recovery have been somewhat neglected in reservoir management. Drainage and imbibition mechanisms occur according to the regional wetting characteristics. Due to the wettability heterogeneities, miscible and immiscible flow will have completely different displacement patterns, as will be shown later in this paper. However, oil recovery is a function of the reservoir conditions including the effects of these heterogeneities, so must be honoured when making realistic field simulations.

2 The problems of preparing the geological models for reservoir flow modelling

A problem confronting all hydrocarbon reservoir modellers is how to represent the heterogeneities of a reservoir in a number of grid blocks acceptable to the CPU capacity of the computing facility, and then how to get the representation of the physical effects right. The simulation model must capture reservoir geometry, internal architecture, rock properties and their variability, fluid content, properties and their distribution as well and these effects on the fluid displacement patterns. The initial geological model upon which the simulation model is based is usually much more detailed than the flow model because the flow equation calculations require much time to compute, and therefore a smaller number of grid cells have to be used. Often the number of grid blocks for the geological model has to be reduced from its original 1–10 million grid blocks by up to a factor of 10 to accommodate the solution of the equations of motion of the fluids (Stern 2005). Thus for a reservoir of size say $10\,\text{km} \times 4\,\text{km} \times 100\,\text{m}$ maybe the 10,000,000 grid blocks for the geological model are reduced for the reservoir simulation flow model into $500 \times 100 \times 20$ units so making each grid block of size $20\,\text{m} \times 40\,\text{m} \times 5\,\text{m}$. These blocks are assumed homogeneous but, in reality, most geological reservoir features will have changed over these types of dimensions, and such changes can have a dramatic affect on reservoir flow performance.

Unless the heterogeneities within the reservoir are 'known' or at least recognised in some way, and their effects on displacement honoured, the results of computer simulation of the reservoir from core tests will be uncertain. Sometimes the real flow can be grossly distorted, particularly at the nodes of permeability contrasts (points at which permeability changes discontinuously in more than one coordinate direction), so that the flow will not be aligned with the principal axes (crossflow) (Lambeth and Dawe 1987, 1988). Effects of 'model' heterogeneities on displacement can help this recognition.

Representing a heterogeneous body by a homogeneous one that is macroscopically 'equivalent in some sense' to the original is carried out by upscaling, averaging and upgridding (King 1996; Renard and de Marsily 1997; Shaw and Dawe 1985, 1987; Stern 2005; Lu and Bao 1992). The problem is how to reduce the number of grid blocks, termed 'upscaling', but keep the major features of the displacement patterns. Any averaging method is unlikely to give flow patterns and fluid production that match reality; they will give only average flows. Nowadays, the parameters such as relative permeability, nonlinear dispersion terms, effective retention functions or capillary pressure (and which are themselves all saturation dependent), derived from interpretations of core displacement tests, are used at upscaled reservoir grid block dimensions. These may be unreliable if heterogeneities are present within the tested core, and as a consequence the derived parameters will probably be incorrectly representing the processes for oil recovery and water control techniques at the scaled-up reservoir size (scale-up). Experimental evidence in well-defined heterogeneities can be used as a benchmark to test up-scaling methods, and guide the modellers to verify simulation predictions.

3 Quadrant model

A simple heterogeneous model is the 2×2 block, the checkerboard or quadrant model, shown in Fig. 1, where k is the block permeability (King 1996). Recently, Yeo and Zimmerman (2001) discussed the numerical problem of how to represent the heterogeneities of a reservoir with a number of grid blocks acceptable to the CPU capacity of the computing facility. They found that 'there is significant error even for miscible single phase, constant viscosity flow as the permeability contrast between the permeability blocks increases'. The fluid displacements at the boundaries become simple outflows whereas, as will be shown, practically they do not exit uniformly at the outlet boundary. Yeo and Zimmerman (2001) show that renormalisation errors become significant (>10%) as the conductivity ratio, k_2/k_1 grows ($k_2 > k_1$).

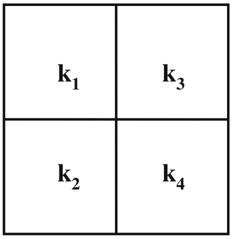

Fig. 1 The quadrant model—the general case is where the properties of blocks 1–4 vary. We consider here cases where $k_1 = k_2 = k_3 = k_4$ (the uniform base case); the permeability case is where $k_1 = k_4$ and $k_2 = k_3$; and the wettability case is where $k_1 = k_2 = k_3 = k_4$, but the wettability of blocks 1 and 4 are the same (water-wet) but opposite to those of blocks 2 and 3 (oil-wet)

This linear quadrant-model (chequer board) combines layering and cross bedding that occurs frequently in reservoirs. If present in a core or reservoir body, its effects on displacement should be accounted for in displacement calculations. Both permeability and wettability contrasts can be implicated. The quadrant model illustrates what might occur during displacement

- if a layered system (common to many reservoirs) were subject to faulting, where adjacent rock sections now have different permeabilities,
- when sedimentary rocks contain patches of different permeability, or wettability (a lens system),
- a wellbore has near-wellbore flow patterns modified due to damage, such as filtrate invasion, inconsistent acidisation along the wellbore, fines blocking or even the effects of perforation,
- in simulators where adjacent grid blocks have different permeabilities,
- in experiments where cores have been butted together to get a suitable length, but the cores have laminations which are not now continuous due to the butting.

The effective permeability of the quadrant model was first investigated by Cardwell and Parsons (1945) who showed that its combined permeability is not a simple average, but lies between the volume weighted arithmetic average and harmonic mean of the constituent permeabilities. Yeo and Zimmerman (2001) discuss the different averaging procedures in more detail and show their limitations, and simulate unit mobility miscible displacement flow patterns. They show that simple analysis as given in the textbooks for averaging parallel or series flow cannot be applied. Unfortunately, these equivalent permeabilities do not give any guide as to the flow patterns that may occur within the model.

This paper explores an individual quadrant heterogeneity model, both by permeability and by wettability, and demonstrates that the flow behaviour, even for miscible flow is complex and will be difficult to simulate. We discuss some displacement experiments carried out using carefully prepared permeability and wettability heterogeneous quadrant model beadpacks. These experiments provide visual evidence of the processes occurring within such porous media, and could be a valuable verification tool and a calibration data source for those investigating upscaling or renormalisation modelling procedures, or wishing to simulate the effects of capillary pressure under different wettability conditions under controlled heterogeneity. The possible loss of physical reality of the displacements must always be considered, particularly the implications for those computing effective conductivities for numerical reservoir simulation.

4 Experimental procedures

A two-dimensional, rectangular sealed plexiglass box (internal diameter 20 cm × 10 cm × 0.6 cm) filled with glass beads was used to carry out the flow studies. Permeability contrasts were achieved by using different grades of glass ballontini beads, grades 9 and 6 (diameters 310–425 and 640–750 μm, respectively) giving a permeability contrast of 2.5. The beads were normally water-wet. The beads could be chemically treated with a water repellent (dimethydichlorosilane) to make them oil-wet. For the wettability experiments presented here water- and oil-wet grade 9 beads were used.

The porosity of the glass beads was determined gravimetrically and found to be $40 \pm 2\%$, for both grades of bead. The absolute permeability of the beads was experimentally measured by means of the falling head method and found to be 110 and 270 Darcy, respectively. The pore volume was approximately 48 ml. Further details are available (Caruana 1997; Caruana and Dawe 1996a, b).

The main packing procedure was to place very thin cardboard barriers inside the box, at the positions of the separate zones of different properties. The models were filled with appropriate beads and vibrated at 100 Hz to help settle the beads and ensure uniform packing. The barriers were then carefully withdrawn. After dry packing, carbon dioxide was passed at low pressure through the packed bed to displace the air. Degassed water was then pumped at constant rate which displaced and absorbed the carbon dioxide (all aqueous fluids were degassed by vacuum before use). Each beadpack was checked for uniform packing, particularly at the edges with the box walls, as edge effects would distort the flow and hence conclusions. Any model that showed ‘edge effects’ was discarded and the packing redone. Details about the fluids physical properties, relative permeability and capillary pressure for beadpacks can be found elsewhere (Lambeth and Dawe 1987; Caruana 1997; Muggeridge et al. 2004).

The fluids were pumped through the models at a constant rate (between 0.05 and 5.0 ml/min) by a pump (Altex 100) through suitable pipework and valves via a number of inlets, as indicated in Fig. 2. Uniform displacement fronts were obtained, and verified by using volumes of coloured fluid. The capillary number for immiscible displacements, defined as $N_{ca} = Q\mu/(L\sigma x)$, where Q = injection rate (ml/s), μ = displacing fluid viscosity (Poise, Pa.s), L = width of the porous medium (cm), x = depth of model (cm), and σ = interfacial tension (mN/m), was of the order of 10^{-6} for a flow rate of 1 ml/min, and which is typical for normal reservoir conditions.

Streamlines were created in some displacements by injecting dyed fluids through septa in the top of the model. Septa were made by drilling small holes and filling them with silastic rubber compound and a syringe needle inserted. Figure 2 shows a schematic of the experimental set-up and Fig. 3 shows how the streamline experiments were carried out.

The mobility ratio for immiscible displacements is the ratio of displacing and displaced mobility, where mobility is itself the ratio of relative permeability at end point conditions and the viscosity of the continuous fluid, i.e. $\mathrm{MR}_{\mathrm{immiscible}} = (\mu_{\mathrm{displaced}} k_{\mathrm{displacing}})/(\mu_{\mathrm{displacing}} k_{\mathrm{displaced}})$. For miscible systems the relative permeability for both phases is the same and so $\mathrm{MR}_{\mathrm{miscible}} = \mu_{\mathrm{displaced}}/\mu_{\mathrm{displacing}}$. Unit mobility

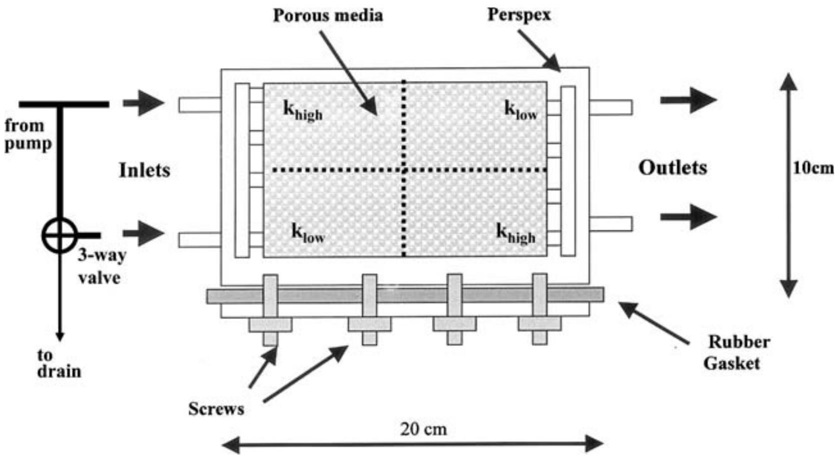

Fig. 2 Schematic of the beadpack equipment

Fig. 3 Schematic of streamline injection arrangement (Caruana and Dawe 1996a). (Figure reproduced with kind permission of Springer Science and Business Media)

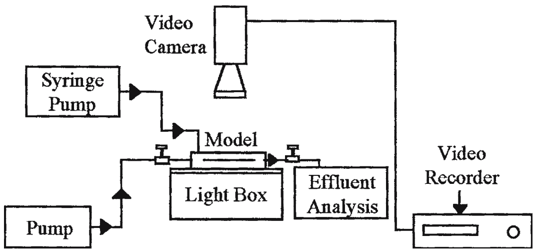

ratio is where MR = 1. For the displacement experiments with viscosity differences (different mobility ratio) the water viscosity was varied by using matched density aqueous solutions of sodium chloride and glycerol (matched density avoided any complicating effects due to density gradients). Mobility ratios for miscible displacements (the ratio of the viscosity of displaced fluid over the displacing fluid, with >1 which gives unfavourable inefficient displacements, and <1 which gives favourable efficient displacements i.e. MR = $\mu_{\text{displaced}}/\mu_{\text{displacing}}$) in the range 0.4–2.5 were used.

For immiscible two-phase displacements, oil/water systems were used. The oil was paraffin with a density of 0.7918 g/cm^3 and a viscosity of 1.4 cp at 20°C. Its viscosity was modified by adding heavy paraffin (BDH, approximately 50 cp) to the paraffin. Any slug displacements were performed by changing the injected fluid after the requisite fraction of pore volume had been metered into the model. In these slug experiments we did not change the fluid viscosity, just the colour, so that we could see internal movements within the bulk fluid. We changed the colour at intervals, usually after some 10–20% volume of the model pore volume had been injected (approximately 5–10 ml).

Dyed tracers were used to follow the displacing and displaced phases as well as for the streamlines. The dyes were chosen so that visual differentiation between the two phases and the streamlines was possible, and gave a good contrast. Water was dyed using Lissamine dyes (red and blue) and oil using Waxolene oil soluble dyes. The displacements were observed by following the movements of the fluid and were recorded by sequence video.

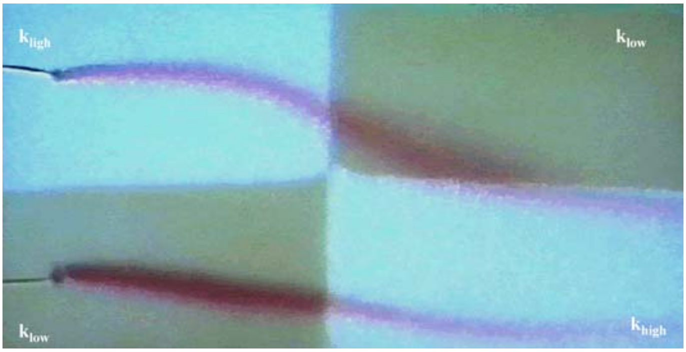

Fig. 4 Streamlines for flow through the quadrant permeability model at unit mobility ratio and a flow rate of 0.8 ml/min

5 Results

The physical processes occurring during fluid miscible and immiscible flow and displacement within glass bead packs having carefully controlled permeability and wettability quadrant models have been studied experimentally. The pattern studied had the quadrants 1–4 of Fig. 4, with quadrants 1 and 4 and 2 and 3 having identical properties, either in permeability or wettability.

First, a full suite of unit mobility miscible displacement flow experiments was carried out (Fig. 5). The actual flow patterns, including streamlines, obtained when flowing through a quadrant geometry were recorded. Then the effects of mobility modifiers were considered with a 20% pore volume coloured displacement slug volume followed by colourless fluid of the same viscosity, and finally the increased problems when immiscible displacements are occurring within permeability (but constant wettability) or wettability (but constant permeability) heterogeneity are demonstrated, both in new photographs and in summarised sequences.

The experiments described below during waterflooding and oilflooding displacements in models having wettability or permeability variations require a consideration of the capillary pressure:

$$p_c = p_o - p_w = 2\sigma \cos\theta / r,$$

where p_o = oil phase pressure, p_w = water phase pressure, σ = interfacial tension, θ = contact angle ($\theta < 90°$, water-wet, $\theta > 90°$, oil-wet), r = pore radius.

In models having wettability variations but constant permeability (r is constant), the capillary pressure decreases as the contact angle increases, therefore, $p_{c(ow)} < p_{c(ww)}$, where the subscripts ow and ww refer to oil-wet and water-wet, respectively. So for either water-wet or oil-wet regions,

$$p_{o(ow)} - p_{w(ow)} < p_{o(ww)} - p_{w(ww)}.$$

The wettability boundary perpendicular to the flow direction creates a capillary pressure contrast which forces the flow towards the node between alternate wettability regions. Before a waterflood, the initial oil phase pressure is uniform throughout the model so $p_{o(ow)} \approx p_{o(ww)}$, and $p_{w(ow)} > p_{w(ww)}$. Therefore water preferentially fills the water-wet regions as the water phase pressure in these regions is lower than that in the oil-wet regions. Similarly, during an oilflood in a water/oil system having wettability variations but constant permeability, the oil would preferentially fill the oil-wet regions as the oil phase pressure in these regions is lower than that in the water-wet regions.

Permeability differences are often differences in pore size and hence will create capillary pressure differences, hence, as there is water saturation difference at the boundaries, there will be capillary pressure differences at these boundaries (Dawe and Grattoni 1998). Petroleum engineers usually model these effects through relative permeability–water saturation formulations (Stern 2005), but they should be slightly different for permeability and wettability differences because the creating physical processes are slightly different. For NAPL applications the capillary pressures may be represented by nonlinear dispersion terms or effective retention functions (Chevalier and Petersen 1999).

5.1 Miscible displacements

5.1.1 Unit mobility displacements

Unit mobility miscible displacements were carried out. The streamline patterns even with a modest permeability contrast, here we have 2.5, are distorted and not aligned with the source-sink axis (Fig. 4). Diagonal flow through the centre of the quadrant leads to streamline distortion to keep the flow within the higher permeability regions and creates a large pressure sink within this central region. It shows a full suite of displacements (rather than the single frame given in Lambeth and Dawe 1987). Clearly the streamlines become distorted as the flow moves to pass through the quadrant join. This links the principle source-sink axis and follows the paths of lowest potential.

Figure 5 presents a typical sequence of a unit mobility displacement. A distinctive tongue can clearly be observed. Early fluid breakthrough occurs in a part of k_4(a higher permeability quadrant). Nodal flow effects occur as the flow moves towards the centre of the model. The flow becomes channelled through the area where the four quadrants meet. Some flow naturally has to pass through the lower permeability areas of zones 2 and 3.

5.1.2 Miscible non-unit mobility displacement

Experiments were then carried out to observe the flood front patterns for favourable and unfavourable displacements. The viscosity of the displacing and displaced fluids was varied so that the ratio ranged between 0.4 and 2.5 (NB. viscosity and mobility ratio are the same for miscible displacements). Figure 6 shows the fluid movements within the tongue as simulated (Lambeth and Dawe 1987; Yeo and Zimmerman 2001). Figure 7 shows schematically favourable, unit (displacing and displaced fluids have the same viscosity) and unfavourable displacements. Here we represent the displacement pattern by a slug of 'black fluid' (~20% pore volume) displaced further by white fluid with the same viscosity (i.e. a unit mobility displacement within this slug). The distortions of the displacement continue because of the quadrant geometry. Even with modest conductance contrast (2.5) (conductance ratio in this work can be taken as permeability ratio), and for favourable displacements, very early breakthrough occurs in the quadrant model at k_4 and sweep efficiency is poor, Fig. 7a. The length and width of the tongue are functions of the mobility ratio, conductance contrast and

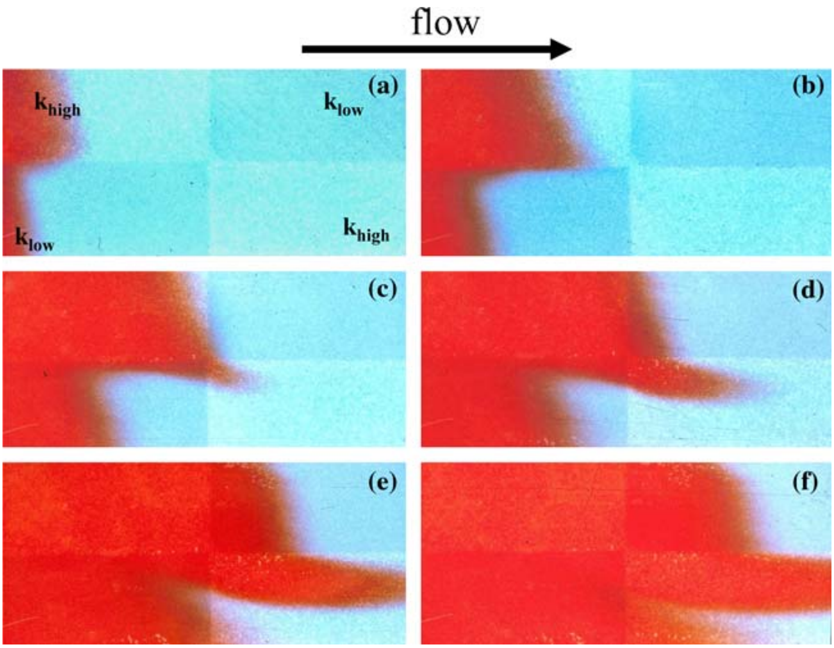

Fig. 5 Unit mobility displacement in the permeability case where $k_1 = k_4$ and $k_2 = k_3$ with a 2.5 permeability ratio and a flow rate of 1.0 ml/min

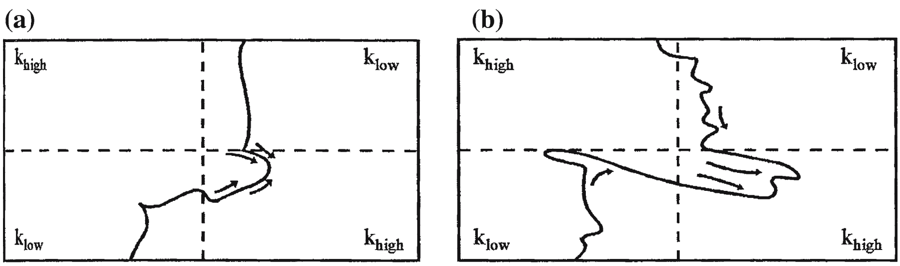

Fig. 6 Floodfront patterns for (**a**) favourable and (**b**) unfavourable, displacement mobility ratio

time; for a given conductance contrast and volume of fluid injected, the tongue length and hence breakthrough time is proportional to the mobility ratio. The width of the tongue clearly will be dependent on the conductance contrast. Some viscous fingering occurred in the low permeability regions, Fig. 7c, but this will always be a secondary effect and can be neglected in any initial analysis.

5.2 Immiscible displacement

Our immiscible displacement experiments show visually the effects due to capillary pressure differences and wettability heterogeneities on the oil and water flow, oil recovery and residual oil. Results are reported here for both waterfloods and oilfloods at low injection rates (<1 ml/min). We give demonstration photographs, but the

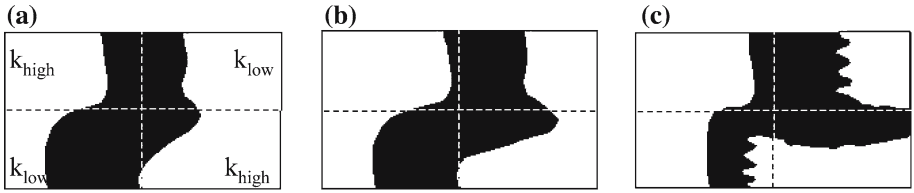

Fig. 7 The effect on miscible displacement patterns of viscosity modifiers, where the displacing and displaced fluid viscosities have ratios of 0.5, 1 or 2. The trailing edge shows the general displacement pattern behind the front. (**a**) favourable, (**b**) unit and (**c**) unfavourable mobility ratio

displacement fronts have been drawn from the sequence photographs in some figures to show more clearly the displacement fronts and streamlines.

Two types of immiscible experiments were carried out.

a. The quadrants had different permeabilities; quadrants 1 and 4 had size 6 beads and quadrants 2 and 3 had size 9 beads,
b. The same sized beads were used for each quadrant (size 9) but the quadrants 1 and 4 were water-wet and 2 and 3 were oil-wet.

When the water saturation within the different quadrants drops below 100% saturation, for either permeability or wettability models, relative permeability and capillary pressure phenomena come into play and create complex patterns. In water/oil displacements, drainage and imbibition mechanisms occur according to the regional wetting characteristics and the saturation change direction. Drainage is increase of non-wetting phase saturation; imbibition is increase of wetting phase saturation. Also the displacement patterns are different for wettability contrasts and for permeability contrasts. The physics is difficult to isolate and interpret clearly due to the various interactions. The boundary perpendicular to the flow direction will create a capillary pressure difference and thus a saturation contrast, so will create extra pressure differences which will further modify the flow through the node between the two alternate quadrants.

5.2.1 Permeability contrast

5.2.1.1 Waterflooding (Figs. 8, 9) The model was initially filled with oil. Water was then pumped through the system (Fig. 2). Due to favourable capillary pressure, the water phase pressure in the inlet low permeability region, k_2, caused the water to enter (imbibe into) this quadrant, Fig. 8. The water moved with a stable displacement front within this region and filled it, leaving only irreducible oil behind. The vertical permeability boundary between the inlet low permeability and outlet high permeability regions caused a restriction to the flow of water, created by the capillary boundary pressure between the two permeability regions, and as a result, the water inlet pressure increased to overcome this restriction to flow. Figure 9 summarises the whole displacement.

The boundary between two permeability regions creates the difference in capillary pressure ($2\sigma\cos\theta/r$). If it is larger in the finer material than the coarser, it will create a resisting barrier effect to flow at the porous media boundary. Additionally, the capillary pressure difference will change as the saturation changes. Once the boundary pressure had been overcome (by a small leakage at some random point) the local

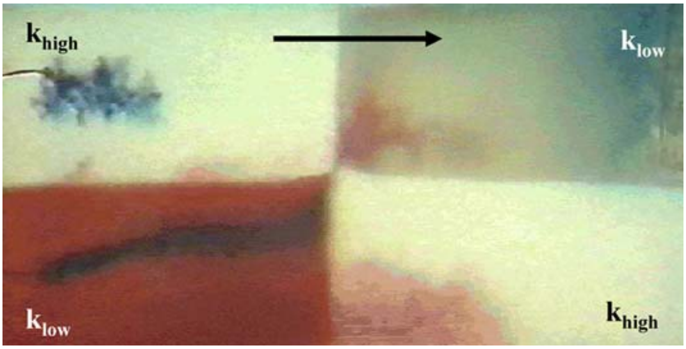

Fig. 8 Waterflooding the quadrant permeability model. Unit mobility immiscible displacement permeability patterns where $k_1 = k_4$ and $k_2 = k_3$ with a 2.5 permeability ratio contrast and a flow rate of 0.5 ml/min. The effects of capillary pressure complicate interpretation, as the displacement patterns are now also saturation dependent

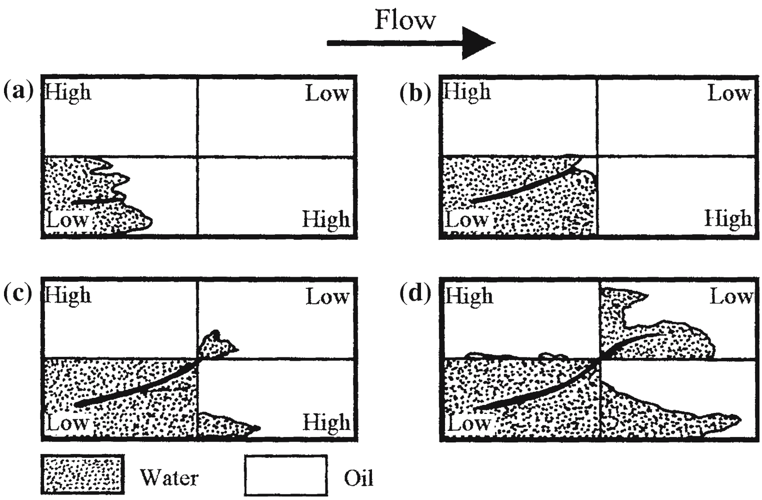

Fig. 9 Summary of waterflooding the quadrant permeability model

water saturation increases and so reduces the local capillary pressure. Water ingress which modifies the local capillary pressure (saturation change) and allows more water to ingress (represented in petroleum engineering simulations by an increase in water relative permeability). Water then flowed through the node, and also across the vertical boundary between the inlet low permeability and outlet high permeability regions. However, most of the flow initially occurred through the node into the outlet low permeability region (as seen by the fluid streamline), because of a favourable water pressure gradient in this low permeability region. At breakthrough, a large amount of oil was left by-passed in the high permeability regions. The inlet high permeability region was left unswept, while only a small portion of the oil in the outlet high permeability region was produced.

5.2.1.2 Oilflooding (Figs. 10, 11) During oilflooding, the quadrant model was initially filled with water. The oil entered the high permeability region and moved

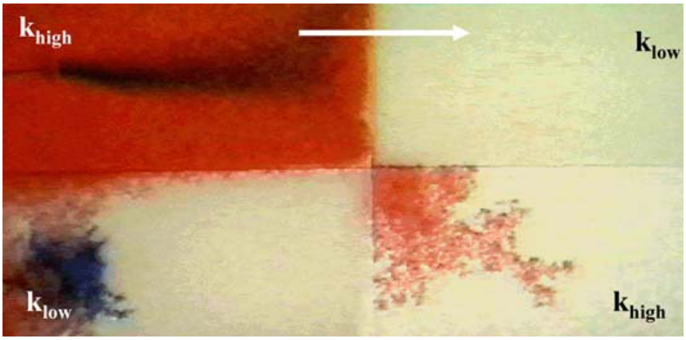

Fig. 10 Oil flooding the quadrant permeability model for a flow rate of 1.0 ml/min

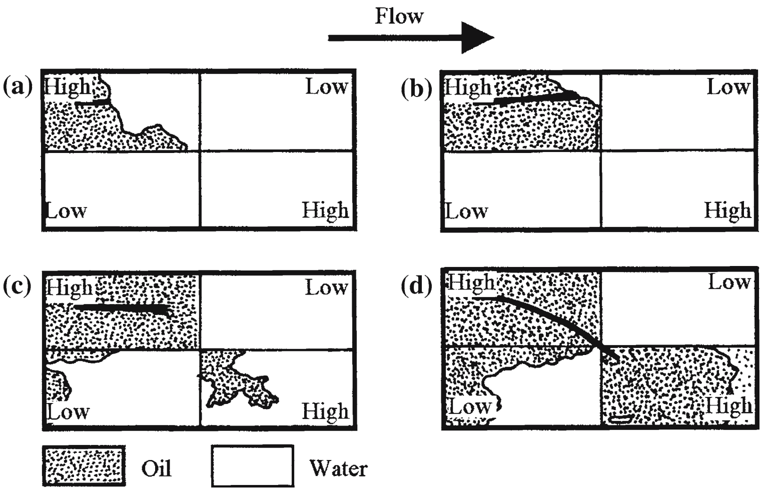

Fig. 11 Summary of oilflooding the quadrant permeability model

steadily within this region with a stable front, while little oil entered the inlet low permeability region, generally in similar, but reversed manner, as the waterflood. The oil filled the inlet high permeability region completely, with the vertical permeability boundary between the inlet high permeability and outlet low permeability regions acting as a barrier to the flow of oil, so allowing only water to flow through it. When the oil inlet pressure increases it can eventually overcome the boundary pressure so that some oil can then enter the low permeability region. It will then flow from the high permeability across the low permeability region towards the outlet. At the same time oil also emerged at a fast rate with a very fingered front through the node into the outlet high permeability region. Flow through the high permeability region was favoured due to a lower oil phase pressure in this region. High water saturation occurred at the outlet end of the model due to end effects. At breakthrough, a large amount of water was by-passed in the low permeability areas. In particular, the outlet low permeability region was left unswept. The displacement is summarised in Fig. 11.

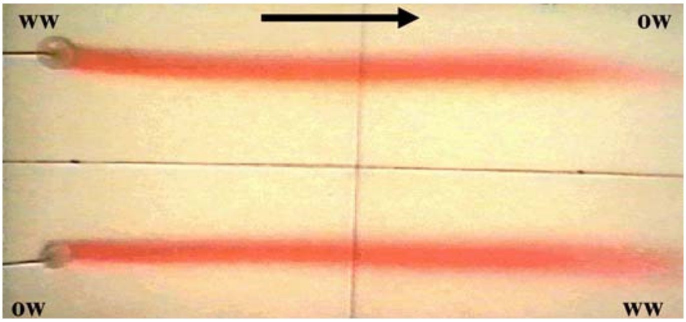

Fig. 12 Water streamlines through wettability heterogeneous model and a flow rate of 0.5 ml/min. Blocks 1 and 4 are water-wet

5.2.2 Wettability contrast

For miscible flow the wettability difference would be expected to have no effect as there is only one phase present in the pores hence no interfacial effects (as we shall show), but during immiscible flow there will be a different behaviour due to capillary pressure reversals. Some wettability contrast experiments have been reported by Caruana and Dawe (1996a). Here we complete the sequences. The first flow experiment in the wettability quadrant was a single-phase waterflood. This is a simple miscible flood. As there are no fluid interfaces (oil/water) no different interactions with the oil- or water-wet beads would be expected by the water. Also the bead pack had a uniform permeability (both sets of beads were grade 9) hence the streamlines are not distorted, Fig. 12.

5.2.2.1 Waterflooding (Figs. 13, 14) The different quadrants have saturation gradients as the displacements proceed and as the fluid saturations drop below 100% relative permeability gradients are created. Also at the boundaries of the water-wet and oil-wet quadrants of the model there are large capillary pressure barriers which can oppose the non-wetting phase entering that block. Figure 13 shows an early stage of the displacement and Fig. 14 summarises the various stages during the waterflooding of the quadrant model. The water entered the water-wet region and no flow occurred in the oil-wet region (Fig. 14a). In the water-wet region the water swept the oil efficiently by an imbibition process and moved with a stable front within this region. Oil was produced via the outlet oil-wet region. The vertical wettability change between the inlet water-wet and outlet oil-wet regions acted as a filter, letting through the oil and holding back the water. When the inlet water-wet quadrant was filled with water (Fig. 14b), the water flowed towards the node and filled up the outlet water-wet region (Fig. 14c). The injected streamlines showed the movement of water within the porous medium. Water breakthrough occurred within the water-wet region at the outlet end of the model and no oil was swept from the oil-wet regions at low rates even after several pore volumes had been passed (Fig. 14).

5.2.2.2 Oilflooding(Fig. 15) The same process as in the waterflood took place during the oilflooding of the quadrant model, but this time it was the oil-wet regions that were efficiently swept by oil imbibition (oil into the oil-wet quadrants), leaving the water by-passed in the water-wet areas even after several pore volumes of oil had been pumped through the model.

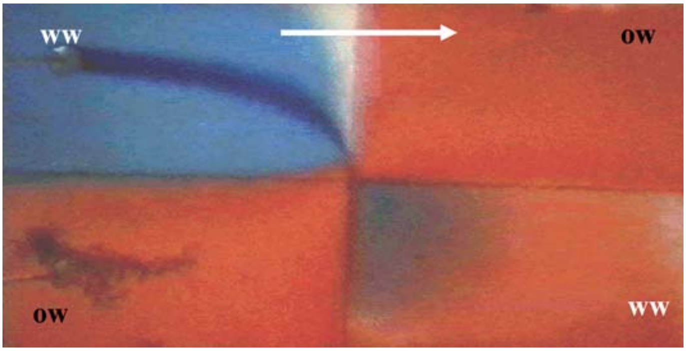

Fig. 13 Waterflooding the quadrant wettability model. The effects of capillary pressure complicate interpretation, as the displacement patterns are now also saturation dependent

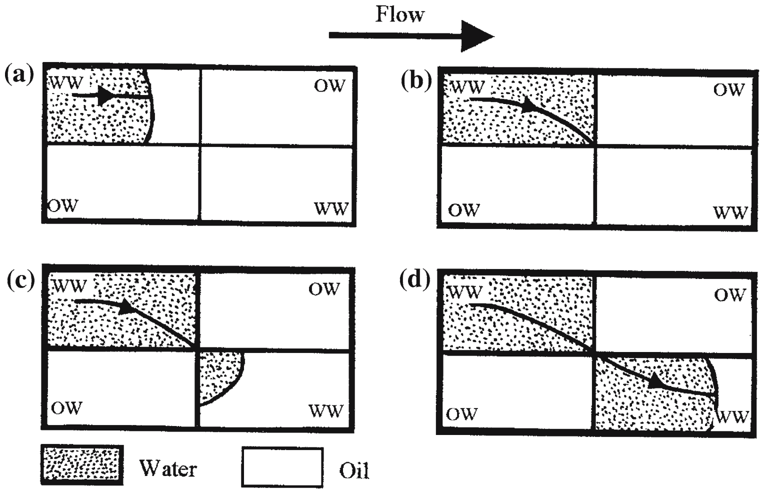

Fig. 14 Summary of waterflooding the quadrant wettability model (Caruana and Dawe 1996a). (Figure reproduced with kind permission of Springer Science and Business Media)

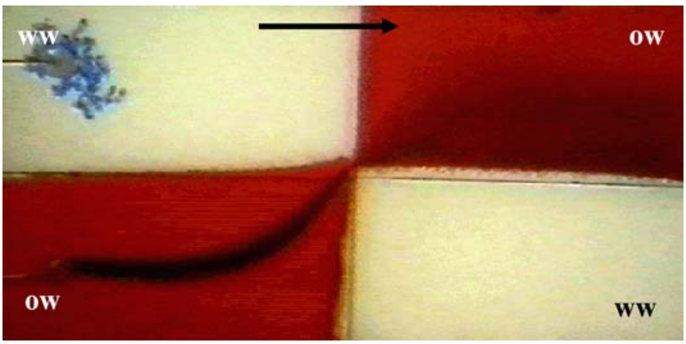

Fig. 15 Oilflooding the quadrant wettability model for a flow rate of 0.5 ml/min

6 Discussion

6.1 Unit mobility simulation

The unit mobility miscible experiments for an individual quadrant have been simulated previously (Lambeth and Dawe 1988; Caruana 1997; Yeo and Zimmerman 2001). Yeo and Zimmerman (2001) discuss the effectiveness of averaging permeability by various procedures (arithmetic, mean and harmonic) and conclude that as the ratio k_1/k_2 moves away from 1 all the averaging techniques becomes inaccurate. They found that getting the same flow patterns was problematic.

Flow vectors are frequently not parallel to the potential sources and sink as the fluid potential gradient originates from viscous forces at any point and is dependent upon the surrounding fluid distributions (Roti and Dawe 1993). These effects are generally greatest where the pressure gradients (and fluid saturations for immiscible displacements) change most rapidly, such as at permeability contrasts (or wettability boundaries or at displacement fronts). These changes cause the fluid displacement patterns to become highly non-uniform, making the prediction of the displacement fronts difficult. How to represent this tonguing by less grid blocks is challenging, particularly because of the rectangular box-like nature of conventional finite difference formulations. Clearly a large number of gridblocks to model such complex flow patterns is required.

Orthogonal curvilinear grids based on the streamlines maybe of benefit provided the nodes and boundaries are well defined. This technique can allow a reduced number of grid blocks to model such systems effectively (Lambeth and Dawe 1988). For example, they compared the computed displacement front using standard Cartesian and curvilinear grids with the experimental data, and found that the form of the central finger was much more accurately modelled by use of the curvilinear grids. However, this methodology was expensive in CPU-time and would not be suitable for incorporation into a general reservoir simulator.

6.2 Immiscible experiments

Clearly, the difficulties are compounded during immiscible displacements as capillary effects and relative permeabilities come into play. For example, for a waterflood displacement there are both imbibition and drainage displacement modes occurring. Imbibition takes place in the water-wet regions when the water saturation is increasing and drainage in the oil-wet regions when the water saturation is decreasing. The water saturation varies throughout a quadrant, and can have a step change at a quadrant boundary. The role of capillary pressure, both at a boundary and within a homogeneous porous medium as the saturation changes is difficult to identify but is needed to represent the various physical process by equations (Caruana 1997; Laroche et al. 1999). How to represent them in these equations has not yet been fully practically solved. Additionally, often a 'breakthrough' through a boundary can only occur by a local pore scale insurgence of one of the fluids into the other. Once this breakdown has occurred, the saturation can change so reducing the capillary pressure difference, and fluid can then readily move forward. How this can be represented by equations is difficult.

6.3 Core flood interpretation

This study has implications for the interpretation of core floods, especially in the assessment of residual oil and estimation of relative permeabilities. In core tests no reference is usually made to the internal structure of the core samples as there is usually no knowledge of the internal structure (although CT scans can give some information), so cores are usually assumed to be homogeneous. If the core contains nodal heterogeneities, nodal flow through the node and quadrant displacement flow may occur. Clearly calculations based on effluent outflow could be erroneous. If there is wettability heterogeneity, oil remains trapped in the oil-wet regions during a waterflood due to capillary forces so creating locations of residual oil within this heterogeneous porous media. Errors in the values of the saturations of the fluids within the core must occur as only average values are available based on the effluent analysis. No real knowledge of the actual placements is usually available, certainly in routine core analysis, so inaccurate conclusions are possible.

6.4 Wellbore implications

The near-wellbore heterogeneities can significantly affect the placement profile of fluids injected or invading the formation. Such effects must be considered in the design and application of treatments to remedy or prevent formation damage (Evans and Dawe 1994). When drilling with over-balanced conditions (e.g., mud filtrate invasion) or when placing remedial fluids into the formation (e.g., scale inhibitors, acid clean-up fracturing fluid operations, etc.) the placements may not be as expected. The fluids will crossflow into the more permeable areas thus not removing the damage from the low permeable zones, or if the fluids are damaging, damaging these more permeable areas further.

6.5 Reservoir simulation

In reservoir simulation adjacent grid blocks with different permeability or capillary pressure properties must set up a quadrant model effect. Simulation does not cope with saturation or permeability discontinuities easily. Great care is needed to ensure that the displacement physics is not lost (Stern 2005). The modeller must be aware of the real physical processes that he has created before his interpretation can be accepted. Again to reduce the number of gridblocks and upscale is a requirement if CPU-time is a limitation. Clearly the displacement patterns reported in this paper can be used to validate the model. A modeller can test his simulation with the general patterns given here and follow-up if necessary with more specific data reported elsewhere (Caruana 1997). Blanket simulation of a reservoir which has quadrant model characteristics by coarse grid blocks will not address the pattern of flow, as large numbers of grid blocks are needed. This is opposite to the requirements of upscaling where the objective is to reduce the number of gridblocks.

7 Conclusions

The physical processes occurring during miscible and immiscible flow and displacement within permeability and wettability quadrant bead pack models have been studied experimentally. The model quadrants 1–4, had 1 and 4 and 2 and 3 with identical properties, either in permeability or wettability.

- Our quadrant model experiments demonstrate that nodal flow occurs for both miscible and immiscible flow, but for immiscible flow there are boundary effects due to capillary pressure differences created by water saturation changes or wettability contrasts which can leave patches of isolated fluid within a quadrant.
- Wettability and permeability heterogeneity lead to different flow displacement patterns for miscible and immiscible flow and give flow patterns often difficult to model. The resulting flow behaviour has not been much discussed in the literature, although it has implications in near-wellbore flow patterns during production and the placement of injection fluids (e.g., for scale inhibition).
- The experimental results presented in this paper, mainly flow pattern pictures, can be used as a benchmark to test up-scaling methods for two-phase flow with permeability or wettability heterogeneity, as well as verification of simulation model predictions using capillary pressure and relative permeability parameters as functions of oil-wet and water-wet media.
- These data have implications for the correct interpretation of core fluid displacement data for scaling-up the processes to reservoir scale (often via relative permeability equations) and for reservoir near-wellbore applications.
- Practically, the knowledge of the fluid movements and flow patterns could assist in the interpretation and remedy of near-wellbore damage.

Acknowledgements We thank Dr. A. Caruana and N. Lambeth for carrying out many of the experiments, Dr. R. W. Zimmerman and Dr. A. Caruana for fruitful discussions, and EPSRC for financial support.

References

Cardwell, W.T., Parsons, R.L.: Averaging permeabilities of heterogeneous oil sands. Trans. AIME **160**, 34–37 (1945)

Caruana, A.: Immiscible flow behaviour in the presence of heterogeneous porous media. PhD thesis, University of London (Imperial College) (1997)

Caruana, A., Dawe, R.A.: Flow behaviour in the presence of wettability heterogeneities. Transport Porous Med. **25**, 217–233 (1996a)

Caruana, A., Dawe, R.A.: Effect of heterogeneities on miscible and immiscible flow processes in porous media. Trends Chem. Eng. **3**, 185–203 (1996b)

Chevalier, L.R., Petersen, J.: Literature review of 2-D laboratory experiments in NAPL flow, transport and remediation. J. Soil Contam. **8**(1), 149–167 (1999)

Dawe, R.A., Grattoni, C.A.: The visualisation of the pore-scale physics of hydrocarbon recovery from reservoirs. First Break **16**, 371–386 (1998)

Evans, R.N., Dawe, R.A.: The danger of neglecting nodal crossflow in heterogeneous near-wellbore conditions. J. Petrol. Sci. Eng. **11**, 113–121 (1994)

King, P.R.: Upscaling permeability: error analysis for renormalization. Transport Porous Med. **23**, 337–354 (1996)

Lambeth, N., Dawe, R.A.: Viscous effects for miscible displacements in regular heterogeneous porous media. Chem. Eng. Res. Des. **65**, 52–62 (1987)

Lambeth, N., Dawe, R.A.: Boundary and crossflow behaviour during displacement in nodal systems, SPE Paper 16972. *SPE Reservoir Eng.* **3**, 1137–1142 (1988)

Laroche, C., Vizika, O., Kalaydjian, F.: Network modelling as a tool to predict three-phase gas injection in heterogeneous wettability porous media. J. Petrol. Sci. Eng. **24**(2–4), 155–168 (1999)

Lu, H., Bao, K.D.: Effective conductivity in a checkerboard geometry at high conductance ratio and high concentration. Phys. Rev. B **46**, 9209–9212 (1992)

Muggeridge, A.H., Jackson, M.D., Agbehi, O., Al-Shuraiqi, H., Grattoni, C.A.: Quantifying bypassed oil in the vicinity of discontinuous shales during gravity dominated flow. *SPE 90402*, SPE Annual Technical Conference and Exhibition, Houston, Texas, 26–29 September (2004)
Renard, P., de Marsily, G.: Calculating equivalent permeability: a review. Adv. Water Resour. **20**, 253–278 (1997)
Roti, Ø, Dawe, R.A.: Modelling fluid flow in crossbedded sections. Transport Porous Med. **12**, 143–159 (1993)
Shaw, D.C., Dawe, R.A.: Perturbation theory for a displacement front passing discontinuities in capillary pressure and permeability in a porous medium. Mathematika **32**, 75–89 (1985)
Shaw, D.C., Dawe, R.A.: Averaging methods for numerical simulations of flows through heterogeneous porous media. Transport Porous Med. **2**, 241–268 (1987)
Stern, D.: Practical aspects of scaleup of simulation models. J. Petrol. Technol. **57**(9), 74–82 (2005)
Yeo, I.W., Zimmerman, R.W.: Accuracy of the renormalization method for computing effective conductivities of heterogeneous media. Transport Porous Med. **45**, 129–138 (2001)